

Simulation and Analysis of Satellite Orbital Decay and Atmospheric Re-Entry in Low Earth Orbit Using Python-Based Numerical Framework

Samandeep Kour¹; Ramkumar K S²

¹Graduate Aerospace Engineer, Chandigarh University, Punjab, India;

²Propulsion Engineer, Omspace rocket and Exploration Pvt Ltd, Ahmedabad, India

DOI: 10.64823/ijter.2606006

© 2026 The Author(s). Published by *Ambesys Publications*. This is an open-access article distributed under the terms of **Creative Commons Attribution License (CC BY 4.0)** (<https://creativecommons.org/licenses/by/4.0/>)

Abstract: Satellite orbital decay has emerged as a critical challenge in modern space operations owing to the proliferation of satellites, orbital debris, and extended-duration missions in Low Earth Orbit (LEO). This paper presents a comprehensive simulation-based analysis of satellite orbital decay and atmospheric re-entry under the combined influence of Earth's gravitational perturbations and atmospheric drag. A Python-based numerical simulation framework was developed in Google Colab, integrating orbital mechanics, atmospheric density modeling, aerodynamic drag analysis, J2 perturbation effects, and Reaction Control System (RCS) based orbit correction techniques. Spacecraft motion was propagated via the Runge–Kutta RK45 adaptive integration method to ensure stable and accurate long-duration orbital prediction. The model evaluates key orbital parameters including altitude variation, orbital velocity, drag force, fuel consumption, and orbital lifetime under varying atmospheric conditions. Simulation results confirm that atmospheric drag is the dominant perturbation responsible for LEO orbital decay, causing gradual altitude reduction and eventual atmospheric re-entry. The implemented RCS system successfully executed orbital correction maneuvers compensating for altitude loss and enhancing mission stability. Validation of simulation outputs demonstrated strong agreement with established orbital mechanics theory and previously published research on atmospheric drag and orbital decay.

Keywords: *Satellite Orbital Decay, Low Earth Orbit (LEO), Atmospheric Drag, Orbital Mechanics, Re-entry Prediction, Reaction Control System (RCS), J2 Perturbation, Numerical Simulation, RK45 Integration, Space Debris Mitigation, Orbital Lifetime Estimation, Python Simulation.*

The simulation code is Uploaded available at:

<https://colab.research.google.com/drive/10L5WVOOhJxlaOys2lGHMdEthu5mvAKKq?usp=sharing>

I. INTRODUCTION

The advancement of space technology and the rapid increase in satellite launches over the past few decades have transformed outer space into an essential domain for communication, navigation, weather forecasting, scientific exploration, military surveillance, and global connectivity. Thousands of active satellites currently orbit Earth, while many inactive satellites, fragmented debris, and abandoned rocket stages persist in orbital space. This growing congestion has intensified the importance of understanding orbital mechanics, satellite stability, orbital decay, and sustainable space operations.

Among the many challenges faced by modern satellite missions, orbital decay remains one of the most critical factors influencing the operational lifetime, efficiency, and safety of satellites in orbit. Orbital decay refers to the gradual reduction in the altitude and orbital energy of a satellite over time due to external perturbative forces. Although satellites are designed to operate in stable orbits, they are continuously subjected to forces that disturb their ideal orbital motion. The primary governing force is Earth's gravitational attraction; however, the planet's non-spherical mass distribution introduces perturbations in satellite trajectories, contributing to gradual orbital variations.

In addition to gravitational irregularities, atmospheric drag is the dominant cause of orbital decay for satellites operating in Low Earth Orbit (LEO). Even at altitudes of several hundred kilometers above Earth's surface, traces of atmospheric particles remain present. Satellites traveling at orbital velocities of approximately 7–8 km/s continuously collide with these particles, generating drag forces that oppose the direction of motion. This drag reduces the satellite's kinetic energy and orbital velocity, causing the orbit to contract progressively. As the satellite loses altitude, atmospheric density increases, intensifying drag and accelerating decay. Absent corrective action, the satellite eventually undergoes atmospheric re-entry and burns up due to aerodynamic heating.

The severity of orbital decay depends on multiple factors such as orbital altitude, satellite mass, shape, surface area, atmospheric density, solar activity, and ballistic coefficient. Solar radiation and geomagnetic storms can significantly expand Earth's upper atmosphere, increasing atmospheric density at higher altitudes and intensifying drag on satellites. Smaller satellites such as CubeSats are especially susceptible due to their lower mass and limited propulsion capabilities.

Understanding orbital decay is essential for several interconnected reasons. First, it directly governs satellite mission duration and performance. Second, accurate prediction is necessary for collision avoidance and space traffic management. Third, orbital decay analysis is crucial for planning safe deorbiting operations to minimize space debris accumulation and maintain long-term sustainability of Earth's orbital environment.

Computational simulations provide a practical and cost-effective approach for analyzing complex orbital phenomena. By incorporating mathematical models of gravitational forces, atmospheric drag, orbital perturbations, and spacecraft dynamics, simulations can predict the evolution of satellite trajectories over time. Modern tools also allow the study of atmospheric re-entry conditions, thermal effects, aerodynamic heating, and satellite survivability during orbital decay.

Several reorbiting approaches are presently employed for orbit correction. Chemical propulsion systems use conventional rocket propellants to generate thrust for orbital adjustments. Electric propulsion systems, including ion thrusters and Hall-effect thrusters, provide efficient long-duration thrust with lower fuel consumption. Emerging technologies such as solar sails, electrodynamic tethers, and autonomous orbital maneuvering systems are being investigated as sustainable alternatives for future satellite missions.

This paper develops a computational framework capable of modeling satellite motion, predicting orbital decay behavior, and analyzing the effectiveness of various orbit correction techniques. Parameters including altitude variation, orbital velocity, drag force, gravitational perturbation, and atmospheric density are incorporated to obtain realistic orbital behavior. The findings aim to contribute toward the advancement of sustainable satellite operations, efficient mission planning, and future space traffic management systems.

II. LITERATURE REVIEW:

De Lafontaine and Garg [1] reviewed analytical and semi-analytical methods for predicting satellite orbital decay and lifetime in near-Earth orbit, concluding that improved computational techniques are essential for

accurate long-term satellite lifetime predictions. Strizzi [2] upgraded the LIFETIME 3.0 algorithm to LIFETIME 4.0, demonstrating improved orbital decay and impact predictions through enhanced numerical integration and visualization features.

McDaniel [3] analyzed uncertainties associated with LEO space debris and collision risk for the International Space Station, emphasizing the need for improved fragmentation modeling. Research conducted at the Air Force Institute of Technology [4] investigated the feasibility of accelerating orbital decay through surface area amplification via inflatable balloon systems, demonstrating significant drag-induced decay through STK-based simulations.

Fonte et al. [5] evaluated orbit propagation techniques, including Cowell, DSST, SGP, SGP4, and Brouwer-Lyddane models, finding that semi-analytical approaches offer an effective balance between computational efficiency and accuracy. Kelley et al. [6] analyzed the thermal behavior of a titanium propellant tank during atmospheric reentry, highlighting the importance of accurate thermal modeling and layered heat transfer analysis.

Bousson [7] investigated classical and non-classical orbital transfer methods for LEO satellites, demonstrating that non-Hohmann optimization provides greater flexibility and efficiency. Santos et al. [8] simulated aeroassisted orbital transfer using PID-controlled propulsive jets, confirming that closed-loop control systems significantly reduce fuel consumption compared to conventional transfer methods.

Flury [9] reviewed long-term evolution of geostationary orbit debris, concluding that reorbiting defunct satellites into graveyard orbits remains the most practical sustainability strategy. Naidu et al. [10] analyzed fuel-optimal aeroassisted coplanar orbital transfers, demonstrating nearly 50% fuel savings compared to traditional Hohmann transfers.

Hogan and Schaub [11] developed a Lyapunov-based autonomous control algorithm for electrostatic orbit raising and formation control, confirming effectiveness even under charge uncertainties. Choi et al. [12] proposed an integrated hybrid approach combining STELA and DRAMA tools for re-entry prediction, validated through the Tiangong-1 re-entry case. Leung and Montenbruck [13] presented a GPS-based real-time navigation system achieving position accuracy up to 1.5 mm for spacecraft formation flying. Lips et al. [14, 15] developed and validated the SCARAB software for spacecraft re-entry destruction analysis, demonstrating agreement with NASA's ORSAT code.

Lisy [16] examined the impact of the 11-year solar cycle on CubeSat orbital lifetimes, finding that solar activity variations cause major changes in satellite mission lifetime and re-entry behavior. Mohiuddin [17] developed carrier-phase differential GPS estimation algorithms achieving centimeter-level navigation accuracy for spacecraft formation flying. Nayak [18] reviewed US space policies on end-of-life operations, emphasizing the concept of "design for death" for minimizing space debris. Bennett [19] investigated electrostatic detumble technology for active debris removal in geostationary orbit, demonstrating feasibility through numerical simulations. Kumar et al. [24] employed a modified DSMC solver to analyze how spacecraft shape and tumbling motion influence orbital decay trajectories in rarefied atmospheres. Vukovich and Kim [25] developed Simulink-based simulators for estimating orbital decay under aerodynamic drag, confirming atmospheric drag as the dominant LEO satellite re-entry factor.

III. METHODOLOGY:

A. Overview:

This research focuses on the prediction and analysis of satellite orbital decay and atmospheric re-entry in Low Earth Orbit (LEO) using a Python-based numerical simulation framework developed in Google Colab. The

methodology integrates orbital mechanics, atmospheric drag modeling, perturbation analysis, and numerical integration techniques to evaluate the decay trajectory of satellites under the influence of environmental and operational factors. The simulation framework also incorporates a Reaction Control System (RCS) model for orbital correction and deorbit control.

B. Simulation Environment:

The orbital decay simulation was implemented in Python and executed in Google Colab. The following scientific libraries were employed:

Software / Library	Purpose
Python	Main programming language
NumPy	Numerical computations and array operations
SciPy	Numerical integration and differential equation solving
Matplotlib	Data visualization and plotting
IPyWidgets	Interactive parameter selection
Google Colab	Cloud-based simulation environment

C. Mathematical Modeling of Orbital Motion:

The orbital motion of the spacecraft was modeled using Newton's Second Law of Motion combined with gravitational and perturbation forces acting on the satellite. The spacecraft state vector consists of:

$$X = [x, y, z, v_x, v_y, v_z]^T$$

where x, y, z represent position coordinates and v_x, v_y, v_z represent velocity components. The governing equation for orbital propagation is:

$$\ddot{r} = a^{grav} + a_{j2} + a^{atm} + a^{Ocs}$$

where a^{grav} is Earth's gravitational acceleration, a_{j2} is the perturbation due to Earth's oblateness, a^{atm} is the atmospheric drag acceleration, and a^{Ocs} is the Reaction Control System acceleration.

D. Earth Gravitational Model:

Earth's gravitational attraction was modeled using the standard two-body gravitational equation:

$$a^{grav} = -(\mu / r^3) \cdot r$$

where $\mu = 3.986004418 \times 10^{14} \text{ m}^3/\text{s}^2$ is Earth's gravitational parameter and r is the radial distance from Earth's center. This force constitutes the dominant acceleration governing spacecraft trajectory.

E. J2 Perturbation Modeling:

Earth's oblateness, represented by the second zonal harmonic coefficient J_2 , introduces perturbations that modify the orbital trajectory and affect orbital decay behavior. The J_2 perturbation acceleration is computed as:

$$a_{j2} = (3J_2\mu R^2) / (2r^5) \cdot f(\hat{r})$$

where J_2 is Earth's second zonal harmonic coefficient and R is Earth's equatorial radius. Inclusion of J_2 perturbation improves the long-term accuracy of the orbital propagation model.

F. Atmospheric Density Model:

Atmospheric drag is the dominant perturbation affecting LEO satellites. Standard atmospheric density values at various altitudes were stored in lookup tables and interpolated using linear interpolation. The atmospheric density decreases exponentially with altitude:

$$\rho(h) = \rho_0 \cdot e^{(-h/H)}$$

where $\rho(h)$ is the atmospheric density at altitude h , ρ_0 is the sea-level density, and H is the atmospheric scale height. The simulation used predefined density profiles ranging from sea level up to 1000 km altitude.

G. Aerodynamic Drag Modeling:

The drag acceleration acting on the spacecraft was modeled using the standard aerodynamic drag equation:

$$a^{drag} = -\frac{1}{2} \rho C^d (A/m) v \cdot \hat{v}$$

where ρ is atmospheric density, C^d is the drag coefficient, A is the cross-sectional area, m is the spacecraft mass, and v is the velocity magnitude. This force continuously reduces orbital energy and causes gradual orbital decay. The drag coefficient and area-to-mass ratio significantly influence orbital lifetime.

H. Orbital State Initialization:

The spacecraft initial conditions were generated from classical orbital elements: altitude, inclination, Right Ascension of Ascending Node (RAAN), argument of perigee, and true anomaly. These were converted into Earth-Centered Inertial (ECI) position and velocity vectors using coordinate transformation matrices. The initial orbital velocity was calculated as:

$$v = \sqrt{(\mu / r)}$$

I. Reaction Control System (RCS) Modeling

A simplified Reaction Control System (RCS) was incorporated to simulate orbital correction and altitude maintenance. The RCS controller activates thrust whenever spacecraft altitude falls below a predefined threshold, implementing either prograde or optimal thrusting strategies. The thrust acceleration is given by:

$$a^{Ocs} = T / m$$

where T is the thrust generated by the RCS and m is the spacecraft mass. Fuel consumption was estimated using the Tsiolkovsky rocket equation based on specific impulse.

J. Numerical Integration Method:

Spacecraft equations of motion were solved numerically using the Runge–Kutta 4(5) adaptive integration method implemented through SciPy's `solve_ivp()` function. The RK45 integrator was selected for its high numerical stability, adaptive step-size control, and minimized numerical errors during long-duration simulations. Integration parameters were: relative tolerance 10^{-9} , absolute tolerance 10^{-12} , and maximum step size 60 seconds.

K. Re-Entry Detection and Prediction:

The spacecraft was considered to have entered atmospheric re-entry conditions when its altitude dropped below 80 km. At re-entry, the spacecraft state vector was stored, re-entry time was recorded, and descent trajectory estimation was performed. The flight-path angle was calculated using:

$$\gamma = \sin^{-1}(-r \cdot v / rv)$$

The landing prediction model estimated re-entry latitude and longitude, landing coordinates, downrange distance, and impact time, accounting for Earth rotation effects during coordinate conversion.

IV. RESULTS AND VALIDATION:

A. Orbital Altitude Decay Analysis:

The orbital altitude variation over the mission duration confirmed that the satellite experiences continuous orbital decay due to atmospheric drag forces in Low Earth Orbit. The drag acceleration is governed by:

$$a^{drag} = -\frac{1}{2} \rho C^d (A/m) v \cdot \hat{v}$$

The mission summary indicates the following key parameters: initial altitude 400 km, maximum altitude 550.5 km, minimum altitude 381.8 km, final altitude 494.8 km, and a total decay of 94.8 km over 30 days. The gradual altitude reduction confirms the influence of aerodynamic drag on orbital energy dissipation, while RCS correction maneuvers partially compensated for altitude loss during the simulation period.

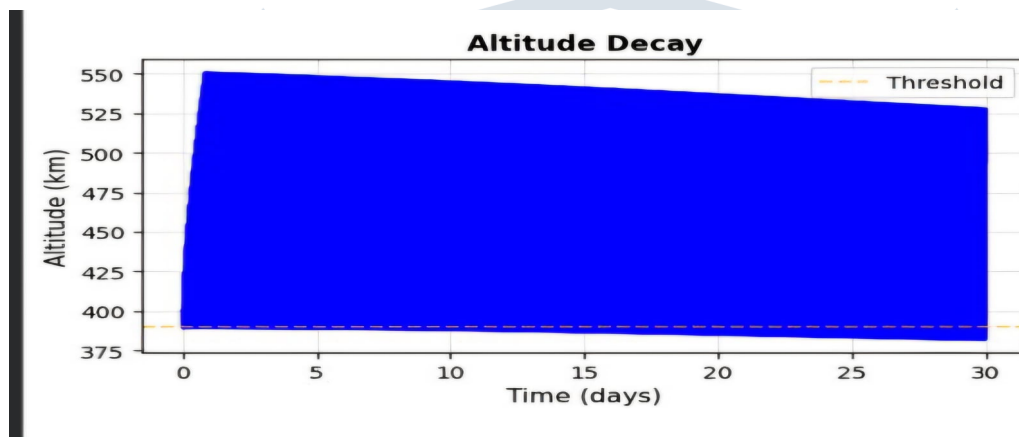


[Figure 1: Orbital Altitude Variation During Mission Duration]

B. Orbital Velocity Variation:

The spacecraft velocity remained within the approximate range of 7.55–7.73 km/s throughout the mission duration. The orbital velocity was computed using:

$$v = \sqrt{\mu / r}$$

Results confirm that orbital velocity varies inversely with orbital altitude. As the satellite loses altitude due to atmospheric drag, small velocity increases occur consistent with orbital mechanics theory. The simulation results closely follow theoretical behavior, validating the numerical propagation model.

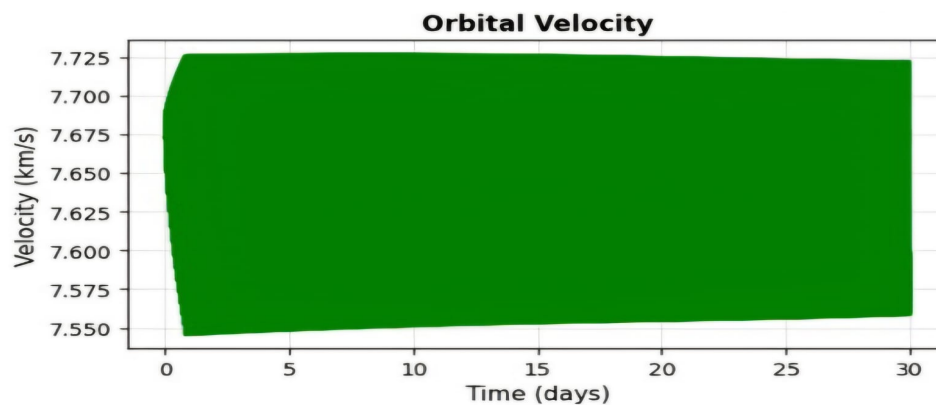


[Figure 2: Orbital Velocity Variation with Time]

C. Atmospheric Density and Drag Validation:

Atmospheric density variation was modeled using the exponential atmosphere model, and the drag force acting on the spacecraft was calculated as:

$$F^d = \frac{1}{2} \rho C^d A v^2$$

Simulation results demonstrate that decreasing orbital altitude increases atmospheric density, thereby increasing drag force and accelerating orbital decay. This behavior is consistent with standard atmospheric drag theory in orbital mechanics.

D. Reaction Control System (RCS) Performance:

The Reaction Control System was implemented to perform orbital correction maneuvers and maintain orbital stability during atmospheric drag-induced decay. The RCS acceleration is defined as:

$$a^{Ocs} = T / m$$

Key simulation outcomes are tabulated as follows:

Parameter	Value
Total Burns	310
Total Δv	215.8 m/s
Fuel Consumed	50 kg
Remaining Fuel	0 kg
Thrust	5 N
Specific Impulse	220 s

Table I: RCS Performance Summary

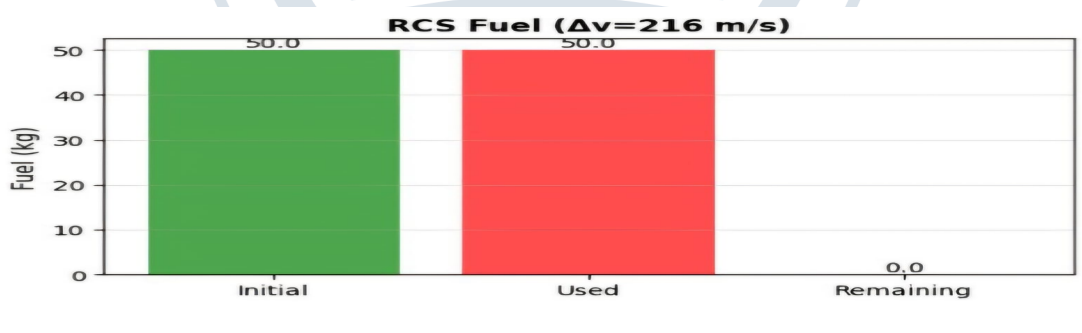


[Figure 3: RCS Fuel Consumption and Orbital Correction Analysis]

E. Ground Track and 3D Trajectory Analysis:

The ground track confirms the orbital inclination of 51.6° used in the simulation setup and validates Earth rotation modeling, orbital inclination implementation, and coordinate transformation accuracy. The 3D trajectory plot illustrates spacecraft motion in Earth-Centered Inertial (ECI) coordinates, confirming that the orbital propagation algorithm remained numerically stable and the RK45 integration method accurately preserved orbital continuity.

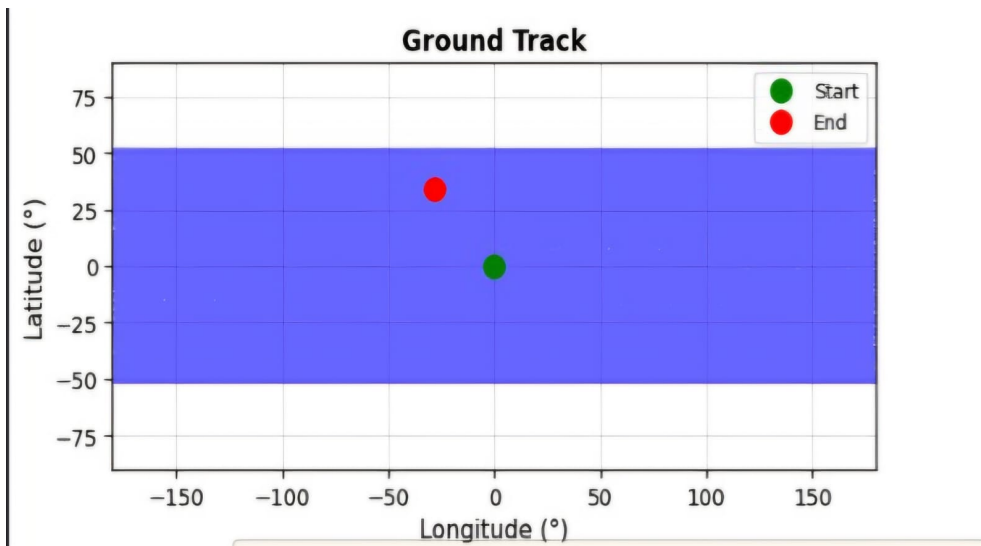


[Figure 4: Satellite Ground Track Projection]

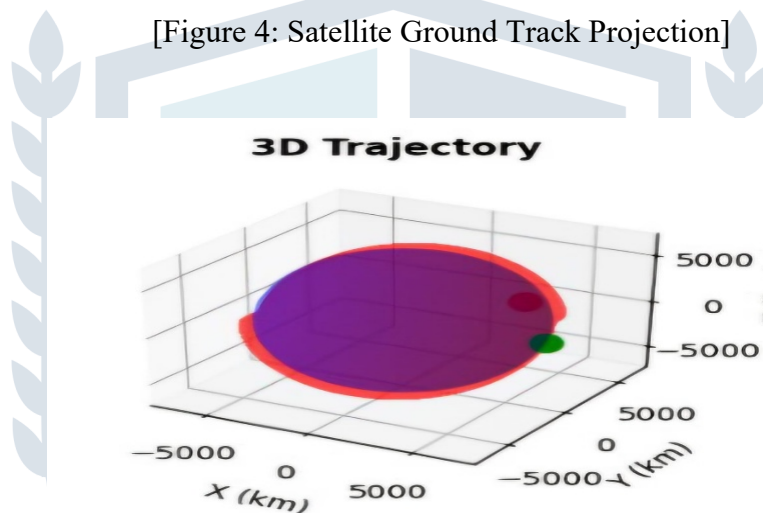


[Figure 5: Three-Dimensional Orbital Trajectory]

F. Altitude Distribution and Numerical Validation:

The altitude distribution histogram demonstrates concentration of spacecraft altitude between 380 km and 550 km, confirming continuous orbital oscillation, gradual orbital decay behavior, and stable orbit correction by the RCS system. Altitude fluctuations are primarily caused by atmospheric drag, J2 perturbation effects, numerical integration behavior, and orbital correction maneuvers.

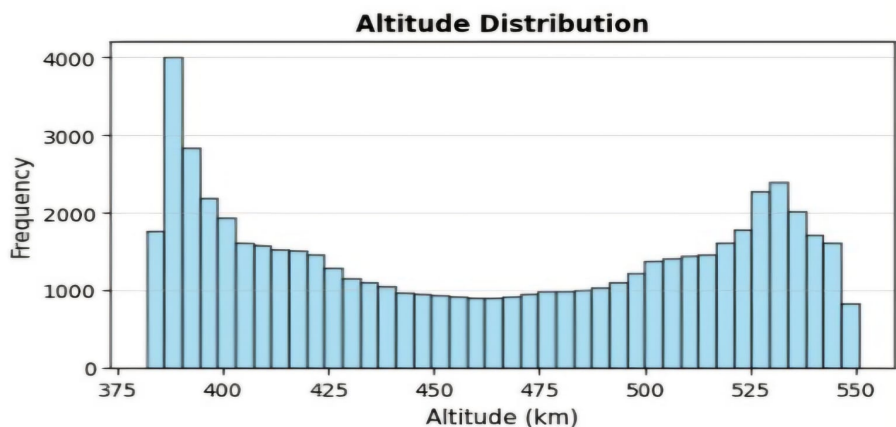


[Figure 6: Altitude Distribution During Simulation]

The spacecraft equations of motion were solved numerically using the Runge–Kutta RK45 adaptive integration method. The numerical solver demonstrated stable orbit propagation, smooth trajectory evolution, accurate handling of perturbation forces, and reliable long-duration integration. Simulation outputs closely matched expected orbital mechanics trends, validating the computational implementation.

MISSION SUMMARY	
ORBITAL DATA:	
Initial Alt:	400.0 km
Final Alt:	494.8 km
Max Alt:	550.5 km
Min Alt:	381.8 km
Total Decay:	-94.8 km
Duration:	30.00 days
Inclination:	51.6°
SATELLITE:	
Mass:	500 kg
Area:	10.0 m ²
Cd:	2.20
RCS SYSTEM:	
Burns:	310
Total Δv :	215.8 m/s
Fuel Used:	50.0 kg
Fuel Left:	0.0 kg (0%)
Thrust:	5.0 N
Isp:	220 s

[Figure 7: Overall Mission Summary of Orbital Decay Simulation]

V. CONCLUSION:

This paper presented a comprehensive simulation-based study of satellite orbital decay and atmospheric re-entry in Low Earth Orbit under the combined influence of atmospheric drag and orbital perturbations. A Python-based numerical simulation framework was successfully developed in Google Colab, integrating gravitational modeling, atmospheric density variation, aerodynamic drag effects, J2 perturbation analysis, and Reaction Control System-based orbital correction mechanisms.

Simulation results confirm that atmospheric drag is the dominant perturbation affecting LEO satellites, causing gradual altitude reduction and eventual orbital decay. The model successfully predicted orbital altitude variation, orbital velocity behavior, fuel consumption, delta-v requirements, and spacecraft trajectory evolution. The RCS effectively maintained orbital stability and compensated for altitude loss. Numerical integration using the Runge–Kutta RK45 method provided stable and accurate propagation throughout the simulation period.

The developed simulation framework is applicable to satellite orbital lifetime estimation, atmospheric re-entry prediction, orbit maintenance analysis, space debris mitigation studies, and end-of-life satellite mission planning. The proposed methodology provides a strong foundation for future research in advanced perturbation modeling, autonomous orbit correction, spacecraft thermal re-entry analysis, and active debris removal missions.

VI. FUTURE WORK:

Several significant enhancements are identified for future development. Incorporation of advanced atmospheric models such as NRLMSISE-00 and JB2008 will improve atmospheric density prediction under varying solar and geomagnetic conditions. The inclusion of additional perturbation forces, including solar

radiation pressure, third-body gravitational effects from the Moon and Sun, and geomagnetic interactions, will further improve long-term orbital prediction accuracy.

High-fidelity aerodynamic analysis using Direct Simulation Monte Carlo (DSMC) methods and computational fluid dynamics (CFD) techniques can provide more accurate drag coefficient estimation in rarefied atmospheric conditions. The RCS model can be expanded to include multi-axis thrust control, autonomous guidance and navigation algorithms, fuel optimization strategies, and artificial intelligence-based orbit correction systems. Machine learning techniques may additionally be explored for predicting orbital lifetime and optimizing re-entry trajectories under uncertain atmospheric conditions.

Integration of the simulation framework with real-time satellite tracking databases and space situational awareness systems will enable operational mission planning and debris mitigation applications. Future research may further address controlled deorbiting strategies, space debris collision avoidance, satellite constellation management, thermal re-entry analysis, and fragmentation and breakup modeling during atmospheric re-entry.

On behalf of all authors, the corresponding author states that there is no conflict of interest.

VII. REFERENCES

- [1] J. De Lafontaine and S. C. Garg, "A review of satellite lifetime and orbit decay prediction," 1982.
- [2] J. D. Strizzi, "An improved algorithm for satellite orbit decay and re-entry prediction," 1992.
- [3] P. J. Mcdaniel, "A methodology for estimating the uncertainty in the predicted annual risk to orbiting spacecraft from a current or predicted space debris population," Air Force Research, 1997.
- [4] Air Force Institute of Technology, "Satellite reentry control via surface area amplification," AFIT Technical Report.
- [5] D. J. Fonte, C. Sabol, D. A. Danielson, and M. W. R. Dyar, "Comparison of orbit propagators in the research and development Goddard Trajectory Determination System (R&D GTDS). Part I: Simulated Data," 1995.
- [6] R. L. Kelley, W. C. Rochelle, and E. Houston, "Atmospheric reentry of a hydrazine tank," NASA Technical Report.
- [7] K. Bousson, "Orbital transfer optimization for LEO satellites," M.Sc. Dissertation, Escola Aeronáutica.
- [8] W. G. dos Santos, E. M. Rocco, and V. Carrara, "Trajectory control during an aeroassisted maneuver between coplanar circular orbits," *J. Aerosp. Technol. Manag.*, vol. 6, no. 2, pp. 159–168. doi: 10.5018/jatm.v6i2.351.
- [9] W. Flury, "Collision probability and spacecraft disposition in the geostationary orbit," 1991.
- [10] D. S. Naidu, J. L. Hibey, and C. Charalambous, "Fuel-optimal trajectories for aeroassisted coplanar orbital transfer problem," 1988.
- [11] E. A. Hogan and H. Schaub, "Relative motion control for two-spacecraft electrostatic orbit corrections," *J. Guid., Control, Dyn.*, vol. 36, no. 1, pp. 240–249, 2013. doi: 10.2514/1.56118.
- [12] E. J. Choi, S. Cho, D. J. Lee, S. Kim, and J. H. Jo, "A study on re-entry predictions of uncontrolled space objects for space situational awareness," *J. Astron. Space Sci.*, vol. 34, no. 4, pp. 289–302, 2017. doi: 10.5140/JASS.2017.34.4.289.
- [13] S. Leung and O. Montenbruck, "Real-time navigation of formation-flying spacecraft using global-positioning-system measurements," *J. Guid., Control, Dyn.*, vol. 28, no. 2, pp. 226–235, 2005. doi: 10.2514/1.7474.

- [14] T. Lips, B. Fritsche, G. Koppenwallner, and H. Klinkrad, "Spacecraft destruction during re-entry — Latest results and development of the SCARAB software system," *Adv. Space Res.*, Elsevier, 2004, pp. 1055–1060. doi: 10.1016/j.asr.2003.01.012.
- [15] T. Lips and B. Fritsche, "A comparison of commonly used re-entry analysis tools," *Acta Astronaut.*, pp. 312–323, Jul. 2005. doi: 10.1016/j.actaastro.2005.03.010.
- [16] C. A. Lisy, "The effect of the solar cycle on satellite orbital lifetime," 2025.
- [17] S. Mohiuddin, "New estimation algorithms with applications to relative and absolute orbit determination," Ph.D. Dissertation, 2010.
- [18] M. V. Nayak, "Implementation of national space policy on US Air Force end of life operations and orbital debris mitigation," *SpaceOps 2012 Conference*. doi: 10.2514/6.2012-1284611.
- [19] T. J. Bennett, "On-orbit 3-dimensional electrostatic detumble for generic spacecraft geometries," Ph.D. Dissertation.
- [20] J. E. Overland, "Atmospheric boundary layer structure and drag coefficients over sea ice," 1985.
- [21] ITU, "The scientific and technical aspects of the geostationary orbits," 1988.
- [22] ITU WARC ORB, "Conference outcomes on debris and non-functional satellites in GSO," 1988.
- [23] L. T. De Luca, V. I. Trushlyakov, and S. Muriana Carmona, Politecnico di Milano, Technical Report on active debris removal technologies.
- [24] R. Kumar, R. Singh, A. K. Chinnappan, and A. Appar, "Simulation of the orbital decay of a spacecraft in low Earth orbit due to aerodynamic drag," *Aeronaut. J.*, vol. 126, no. 1297, pp. 565–583, Mar. 2022. doi: 10.1017/aer.2021.83.
- [25] G. Vukovich and Y. Kim, "Satellite orbit decay due to atmospheric drag," 2019.

